

PAPER • OPEN ACCESS

## Energy-level crossings and number-parity effects in a bosonic tunneling model

To cite this article: Davids Agboola *et al* 2018 *J. Phys. B: At. Mol. Opt. Phys.* **51** 145301

View the [article online](#) for updates and enhancements.

### Related content

- [Exact ground-state correlation functions of an atomic-molecular Bose–Einstein condensate model](#)  
Jon Links and Yibing Shen
- [Behaviour of the energy gap in a model of Josephson coupled Bose–Einstein condensates](#)  
A P Tonel, J Links and A Foerster
- [Dynamical phase transition of two-component Bose–Einstein condensate with nonlinear tunneling in an optomechanical cavity-mediated double-well system](#)  
Qing Li, Lei Tan, Jin-Lou Ma *et al.*



**IOP | ebooks™**

Bringing you innovative digital publishing with leading voices to create your essential collection of books in STEM research.

Start exploring the collection - download the first chapter of every title for free.

# Energy-level crossings and number-parity effects in a bosonic tunneling model

Daivs Agboola, Phillip S Isaac  and Jon Links <sup>1</sup> 

Centre for Mathematical Physics, School of Mathematics and Physics, The University of Queensland 4072, Australia

E-mail: [d.agboola@maths.uq.edu.au](mailto:d.agboola@maths.uq.edu.au), [psi@maths.uq.edu.au](mailto:psi@maths.uq.edu.au) and [jrl@maths.uq.edu.au](mailto:jrl@maths.uq.edu.au)

Received 8 March 2018, revised 24 April 2018

Accepted for publication 22 May 2018

Published 19 June 2018



CrossMark

## Abstract

An exactly solved bosonic tunneling model is studied along a line of the coupling parameter space, which includes a quantum phase boundary line. The entire energy spectrum is computed analytically, and found to exhibit multiple energy-level crossings in a region of the coupling parameter space. Several key properties of the model are discussed, which exhibit a clear dependence on whether the particle number is even or odd. Principal among these is a number-parity effect in the quantum dynamics.

Keywords: quantum tunneling, particle number parity, energy-level crossing

## 1. Introduction

The symmetric two-site Bose–Hubbard model has been studied widely for some time [1–6]. The Hamiltonian reads

$$\mathcal{H} = \frac{k}{8}(N_1 - N_2)^2 - \frac{J}{2}(b_1^\dagger b_2 + b_2^\dagger b_1), \quad (1)$$

where

$$[b_i, b_j^\dagger] = \delta_{ij}\mathcal{I}, \quad [b_i, b_j] = [b_i^\dagger, b_j^\dagger] = 0,$$

for  $i, j = 1, 2$ . Above  $\mathcal{I}$  denotes the identity operator, and  $N_j = b_j^\dagger b_j$ . Setting  $N = N_1 + N_2$ , it can be verified that  $[H, N] = 0$ . The model has a simple interpretation through two terms describing particle interactions with coupling  $k$ , and a tunneling process between two wells with interaction strength  $J$ . Without loss of generality we take  $J \geq 0$ . Though it is simple, the Hamiltonian has been successfully used as a model for experimentally realized tunneling phenomena [7].

Several studies have identified a quantum phase transition in the attractive regime  $k < 0$ , using a variety of approaches

including semiclassical methods [8, 9], mean-field approximation [10], entanglement [11–13], fidelity [12, 13], fragmentation [14, 15], NMR simulations [16], and exact results using Bethe ansatz methods [12, 17]. One way to characterize the two phases is through the energy gap between the ground state and the first excited state. Setting  $k = 0$  in (1) it is not difficult to check that the ground-state energy is  $-JN/2$ , and the gap to the first excited state is  $J$ . At the other extreme when  $J = 0$  and  $k < 0$ , the ground state is two-fold degenerate, so the gap is zero. The transition between these extremes is abrupt. Setting  $\lambda = (kN)/(2J)$  the transition takes place at  $\lambda = -1$  [12].

In recent times a generalized version of (1) has been studied which includes a second-order tunneling process [18–20]. The extended Hamiltonian is

$$H = \frac{k}{8}(N_1 - N_2)^2 - \frac{J}{2}(b_1^\dagger b_2 + b_2^\dagger b_1) - \frac{\Omega}{2}((b_1^\dagger)^2 b_2^2 + (b_2^\dagger)^2 b_1^2), \quad (2)$$

where the coefficient  $\Omega$  is the coupling for second-order tunneling. The inclusion of such a term can be justified on physical grounds, but it is often neglected because the coupling  $\Omega$  is much weaker than  $k$  and  $J$  [21, 22]. Nonetheless, the model has been employed [18] to account for the experimental observation of second-order tunneling in the low-particle number limit [23]. Note that equation (2) does not

<sup>1</sup> Author to whom any correspondence should be addressed.



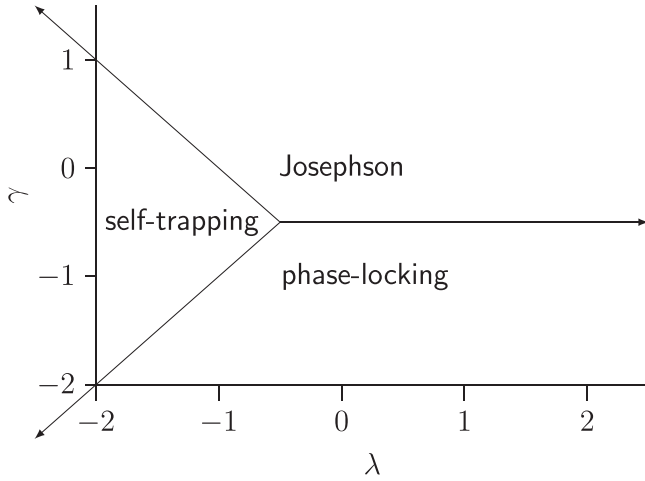


**Figure 1.** Coupling parameter space diagram indicating the three quantum phases identified by bifurcation analysis.

include an interaction term of the form  $N_1 N_2$ , as is found in [18]. Because the total particle number  $N$  is conserved, such an interaction term can be replaced with

$$N_1 N_2 = \frac{1}{4} N^2 - \frac{1}{4} (N_1 - N_2)^2$$

leading to a renormalization of the coupling  $k$  and uniform energy shift within each subspace of fixed  $N$ . This is sufficient for the analysis conducted below, whereby the calculations are performed within subspaces of fixed value for  $N$ .

From the mathematical perspective, (2) offers a richer structure than (1). Analyses of bifurcations of fixed points in the classical limit show there are three expected phases, which will be referred to as *Josephson*, *self-trapping*, and *phase-locking* [19, 20]. The phase-locking phase was studied closely via a classical analysis in [20], where it was highlighted that in this phase two fixed points arise with zero population imbalance and tunable relative phases (different to 0 or  $\pi$ ) as the parameter  $\Omega$  is varied. In this study, it was also found that for the quantum Hamiltonian there occurred multiple energy-level crossings corresponding to this phase, particularly between the ground state and first excited state. Such crossings are a new feature not found in the studies of the Hamiltonian (1)<sup>2</sup>. There is, however, some evidence to suggest that they may be a generic property of systems with non-linear tunneling processes. In particular, this behavior has been observed in models with second-order tunneling between internal degrees of freedom [25–27].

The main objective of this work is to investigate the boundary between the phase-locking and self-trapping phases. Energy-level crossings are also found to occur on this boundary, and they can be precisely identified. The energy levels can be computed analytically. The character of the set of energy levels is dependent on whether the particle number is even or odd. We will study some of the consequences of this finding, which may have implications for few-body bosonic systems.

<sup>2</sup> The conclusion that equation (1) does not have energy-level crossings follows from a mapping of the spectrum into that of a one-body Schrödinger problem. See e.g. [24].

The results complement those for few-body fermion systems, that have attracted recent attention [28, 29]. A significant finding, that goes beyond the results of [18, 20], is a clear sign that the quantum dynamics of the system can display behaviors which are strongly influenced by the number-parity.

In section 2 we begin by establishing that the phase-locking and self-trapping phases exhibit a duality. The boundary between them is a self-dual line with an enhanced symmetry. In section 3 we recall Bethe ansatz equations (BAE) for the model, which are easily solved on the self-dual line. This solution is used in section 4 to examine the nature of the ground-state energy gap, and in section 5 a supersymmetric structure within the model is unveiled. Number-parity effects in the computation of dynamical expectation values are investigated in section 6, and concluding remarks are given in section 7.

## 2. Duality

Set  $\gamma = \Omega N/J$ , and recall  $\lambda = (kN)/(2J)$ . The boundary lines between the three phases, which are identified through bifurcation analysis, are [20]

- self-trapping/Josephson:  $\gamma + \lambda = -1$  for  $\lambda \leq -1/2$ ;
- phase-locking/self-trapping:  $\gamma = \lambda$  for  $\lambda \leq -1/2$ ;
- Josephson/phase-locking:  $\gamma = -1/2$  for  $\lambda \geq -1/2$ .

The three boundaries meet at the triple point  $(\lambda, \gamma) = (-1/2, -1/2)$ . A representation of the phase diagram is given in figure 1.

To reveal the duality between the phase-locking and self-trapping phases, introduce the  $su(2)$  realization

$$S^+ = b_1^\dagger b_2, \quad S^- = b_2^\dagger b_1, \quad S^z = (N_1 - N_2)/2 \quad (3)$$

satisfying the relations

$$[S^z, S^\pm] = \pm S^\pm, \quad [S^+, S^-] = 2S^z, \quad (4)$$

for which the Casimir invariant  $C = 2(S^z)^2 + S^+ S^- + S^- S^+$  has eigenvalue  $\Lambda = N(N + 2)/2$ . In terms of this realization, the Hamiltonian is expressed as

$$H = \frac{k}{2}(S^z)^2 - JS^x - \frac{\Omega}{2}((S^+)^2 + (S^-)^2). \quad (5)$$

This Hamiltonian will now be transformed by a composition of three unitary operators:

$$\begin{aligned} T : S^x &\mapsto -S^z, S^y \mapsto S^y, S^z \mapsto S^x, \\ R : S^x &\mapsto -S^y, S^y \mapsto S^x, S^z \mapsto S^z, \\ U &= T^{-1} \circ R \circ T, \end{aligned}$$

where  $S^x = (S^+ + S^-)/2$ ,  $S^y = (S^+ - S^-)/(2i)$ . Note that  $T$  and  $R$  are rotations of  $\pi/2$  about the  $y$ - and  $z$ -axes respectively, such that  $U^4 = \text{id}$ . It is found that

$$\begin{aligned} U(H) &= \frac{1}{4}(6\Omega - k)(S^z)^2 - JS^x - \frac{1}{8}(k + 2\Omega)((S^+)^2 + (S^-)^2) \\ &\quad + \frac{1}{8}(k - 2\Omega)C, \end{aligned}$$

and  $U^2(H) = H$ . It is easily checked that, up to the inclusion of an  $N$ -dependent term,  $U$  maps Hamiltonians between the

phase-locking and self-trapping phases, while Hamiltonians in the Josephson phase are mapped back to the Josephson phase under the action of  $U$ . This shows that there is a one-to-one correspondence between the energy spectra in phase-locking and self-trapping phases. Hamiltonians on the line  $\gamma = \lambda$ , or equivalently  $\Omega = k/2$ , are invariant under the action of  $U$ . Along this line, which includes the boundary between the phase-locking and self-trapping phases, analytic expressions for the entire energy spectrum can be obtained, as we describe below.

### 3. Exact solution

The Bethe ansatz solution derived in [20] gives the energy eigenvalues and eigenvectors as

$$E = \frac{kN^2}{8} - \frac{J}{2} \sum_{j=1}^N u_j - \frac{\Omega}{2} \sum_{j=1}^N \sum_{k \neq j}^N u_j u_k,$$

$$|\Psi\rangle = \prod_{j=1}^N (b_1^\dagger + u_j b_2^\dagger) |0\rangle.$$

Here, the parameters  $\{u_j: j = 1, \dots, N\}$  satisfy the BAE

$$(J(1 - u_j^2) - k(N - 1)u_j + 2\Omega(N - 1)u_j^3)Q'(u_j) = (\Omega(1 + u_j^4) - ku_j^2)Q''(u_j), \quad (6)$$

where

$$Q(x) = \prod_{j=1}^N (x - u_j). \quad (7)$$

Note that the form (6) is different to the BAE presented in [20], which reads

$$\frac{J(1 - u_j^2) - k(N - 1)u_j + 2\Omega(N - 1)u_j^3}{ku_j^2 - \Omega(1 + u_j^4)} = \sum_{k \neq j}^N \frac{2}{u_k - u_j}. \quad (8)$$

Equations (6) and (8) are equivalent whenever there are no root multiplicities in (7). The more general form (6), which accommodates root multiplicities, will be required for the analysis below.

Hereafter set  $\Omega = k/2$ , which is the self-dual line identified in the previous section. For this constraint the BAE (6) are solved with the choice  $u_j^2 = 1$  for all  $j = 1, \dots, N$ . There are  $N + 1$  solutions where  $q$  of the roots are chosen to take the value  $-1$ , while the remaining  $N - q$  are chosen to take the value  $1$ . This gives a complete set of (normalized) eigenstates

$$|N, q\rangle = \frac{1}{\sqrt{2^N q!(N - q)!}} (b_1^\dagger + b_2^\dagger)^{N - q} (b_1^\dagger - b_2^\dagger)^q |0\rangle,$$

$$q = 0, 1, \dots, N, \quad (9)$$

with the corresponding energies

$$E(N, q) = \frac{J}{2}(2q - N) + \frac{k}{8}(8q(N - q) + 2N - N^2). \quad (10)$$

While the structure of the states and spectrum through (9), (10) is very simple, we can see that the system is non-trivial from the following analysis. Fixing  $J$  in (10), by setting  $E(N, q) = E(N, q')$ , we see that all energy levels corresponding to labels  $q, q' \in \left\{0, 1, \dots, \left\lfloor \frac{N}{2} \right\rfloor\right\}$  will cross at values

$$k = \frac{J}{q + q' - N}. \quad (11)$$

Moreover, energy levels corresponding to  $q$  and  $q' = q + 1$  cross when

$$k = \frac{J}{2q + 1 - N}, \quad (12)$$

which decreases as  $q$  increases. This then implies that for all  $k > J/(1 - N)$ , the label  $q = 0$  corresponds to the ground state, noting that for these values of  $k$  there are no further energy-level crossings for this state. By a similar argument, for all  $k < J/(2\lfloor \frac{N}{2} \rfloor - 1 - N)$ , the label  $q = \lfloor \frac{N}{2} \rfloor$  corresponds to the ground state. For labels  $q = 1, 2, \dots, \lfloor \frac{N}{2} \rfloor - 1$ , the ground state occurs when

$$\frac{J}{2q + 1 - N} < k < \frac{J}{2q - 1 - N}. \quad (13)$$

This is easily seen using standard calculus techniques. In other words, all the ground state energy-level crossings occur from the lowest value  $k = J/(2\lfloor \frac{N}{2} \rfloor - 1 - N)$  up to  $k = J/(1 - N)$ .

The level crossings predicted by our analysis are depicted in figure 2. It can be seen that when  $k = 0$  the energies are equally spaced, e.g. see figure 2(a). This is because the eigenstates in this limit are simply discrete momentum eigenstates. For negative  $k$ , as  $|k|$  increases, a sequence of ground-state level crossings occur. Also for sufficiently large  $|k|$  the energies form a system of bands. When  $N$  is odd the number of energy levels is even, and the energy-level bands occur in pairs  $|N, q\rangle$  and  $|N, N - q\rangle$ , each with separation  $J(N - 2q)$ . When  $N$  is even, however, the number of levels is odd, and there is a single unpaired state, e.g. see figure 2(c). This points towards a prospect for number-parity effects, which will be explored below.

We also remark that from (9), it is straightforward to calculate certain correlation functions. For example, for each  $q = 0, 1, \dots, N$

$$\langle (N_1 - N_2)^2 \rangle = N + 2q(N - q),$$

$$\langle b_1^\dagger b_2 + b_2^\dagger b_1 \rangle = N - 2q,$$

$$\langle (b_1^\dagger)^2 b_2^2 + (b_2^\dagger)^2 b_1^2 \rangle = \frac{N^2}{2} - \frac{N}{2} - 3q(N - q).$$

#### 3.1. Continuum approximation

One straightforward approach to analyze the system is to introduce the variable  $l = q/N$ ,  $0 \leq l \leq 1$ , and treat this as varying continuously. This approximation is expected to be a valid in the limit of large  $N$ . To leading order in  $N$  (10)

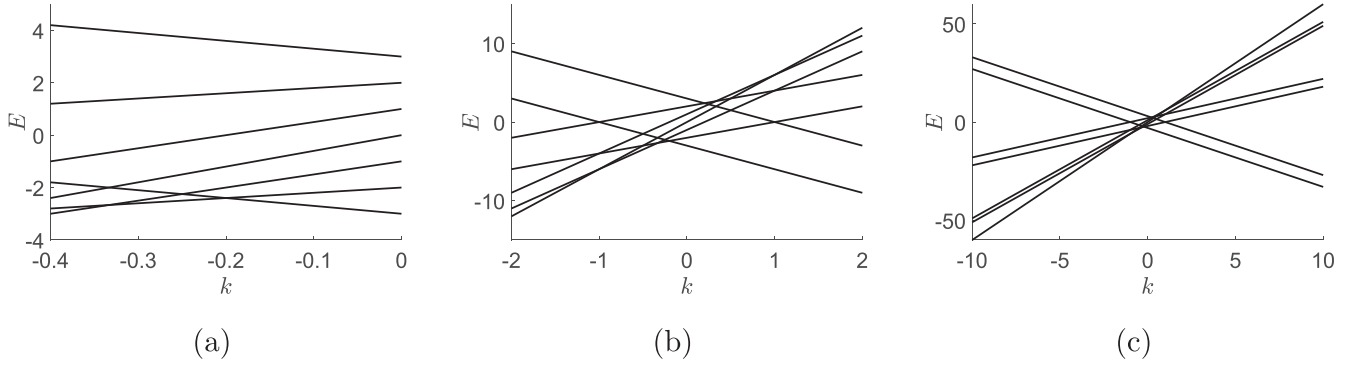


**Figure 2.** Energy levels as a function of  $k$  for  $J = 1$ ,  $\Omega = k/2$  and  $N = 6$ . The figures depict different orders of magnitude for the interval of  $k$ .

becomes

$$E \approx \frac{JN}{4}(4l - \lambda - 2 + 8\lambda l(1 - l)).$$

For  $\lambda \geq -1/2$  the minimum value of energy occurs at  $l = 0$ , while for  $\lambda \leq -1/2$ , the minimum occurs at

$$l = \frac{1}{2} + \frac{1}{4\lambda}. \tag{14}$$

We note that (14) is consistent with (12) in the large  $N$  limit. The following expressions are then found for the ground-state energy and correlations:

$$\frac{E_0}{N} \approx \begin{cases} -\frac{J}{4}(2 + \lambda), & \lambda \geq -\frac{1}{2}, \\ \frac{J}{8}\left(2\lambda + \frac{1}{\lambda}\right), & \lambda \leq -\frac{1}{2}, \end{cases}$$

$$\frac{\langle(N_1 - N_2)^2\rangle}{N^2} \approx \begin{cases} 0, & \lambda \geq -\frac{1}{2}, \\ \frac{1}{2} - \frac{1}{8\lambda^2}, & \lambda \leq -\frac{1}{2}, \end{cases}$$

$$\frac{\langle b_1^\dagger b_2 + b_2^\dagger b_1 \rangle}{N} \approx \begin{cases} 1, & \lambda \geq -\frac{1}{2}, \\ -\frac{1}{2\lambda}, & \lambda \leq -\frac{1}{2}, \end{cases}$$

$$\frac{\langle(b_1^\dagger)^2 b_2^2 + (b_2^\dagger)^2 b_1^2\rangle}{N^2} \approx \begin{cases} \frac{1}{2}, & \lambda \geq -\frac{1}{2}, \\ -\frac{1}{4} + \frac{3}{16\lambda^2}, & \lambda \leq -\frac{1}{2}. \end{cases}$$

The fact that the value of  $l$  as given by (14) is a function of  $\lambda$  is a reflection of the level crossings. It also has the effect of treating the system as being gapless when  $\lambda \leq -1/2$ . While this is correct in some sense, the above treatment does not capture the full physical properties of the model.

#### 4. Ground-state energy gap

Define the ground-state energy gap  $\Delta$  to be the difference between the first excited state energy and the ground-state energy. From previous discussion, we know that for fixed  $J$

and  $q = 1, 2, \dots, \lfloor \frac{N}{2} \rfloor - 1$ , the energy level  $|N, q\rangle$  is the ground state for values of  $k$  given by (13). In the following, we only consider this range of  $k$  and  $q$  values, so that  $|N, q\rangle$  is the ground state. In this case, it is straightforward to show that  $E(N, q + 1) = E(N, q - 1)$  occurs when

$$k = k_p = \frac{J}{2q - N}. \tag{15}$$

The difference in the energy corresponding to  $k_p$  and the ground state is found to be  $J/(N - 2q)$ . Also, the difference in energy between the ground state  $|N, q\rangle$  and the state  $|N, N - q\rangle$  is  $J(N - 2q)$  which is greater than  $J/(N - 2q)$  for the given values of  $q$ . It follows that peaks in the gap must occur at the values  $k_p$  given in (15), corresponding to the crossing of  $|N, q - 1\rangle$  and  $|N, q + 1\rangle$ .

Figure 3 plots  $\Delta$  as a function of  $k$  for  $N = 4, 10, 100$ , and by contrast, figure 4 gives the same plot for odd values  $N = 5, 11, 101$ . For the odd case, the maximum value of the gap is  $J$  for negative values of  $k$ , and for the even case the gap is unbounded as  $k \rightarrow -\infty$ . It is given by  $\Delta = -J - k$  whenever  $k \leq -J$ . Furthermore, these figures illustrate that the gap converges to a ‘sawtooth’ function, however the cases of even  $N$  and odd  $N$  do not converge to the same function. Indeed, the relationship is one in which the locations of the zeros and peaks of the sawtooth functions are interchanged. In both instances the convergence is pointwise, which can be proved rigorously. In neither case, however, is the convergence uniform with respect to the  $\|\cdot\|_\infty$  norm. This is an explicit example of a number parity effect. Note finally that the property that the gap as a function of  $k$  consists of piecewise straight lines is a property of the self-dual line, it does not hold in general. See [20] for example plots of the gap away from the self-dual line.

##### 4.1. Continuum approximation

Figure 5 plots  $\Delta$  as a function of  $\lambda$  for  $N = 5, 11, 101$ . It indicates that the gap vanishes in the limit  $N \rightarrow \infty$ , consistent with the analysis of section 3.1, but the convergence is not uniform. The gapless regime, which occurs for  $k < -1/2$ , arises independently of  $N$  being even or odd. In other words, in the continuum approximation, the number parity effect is lost.

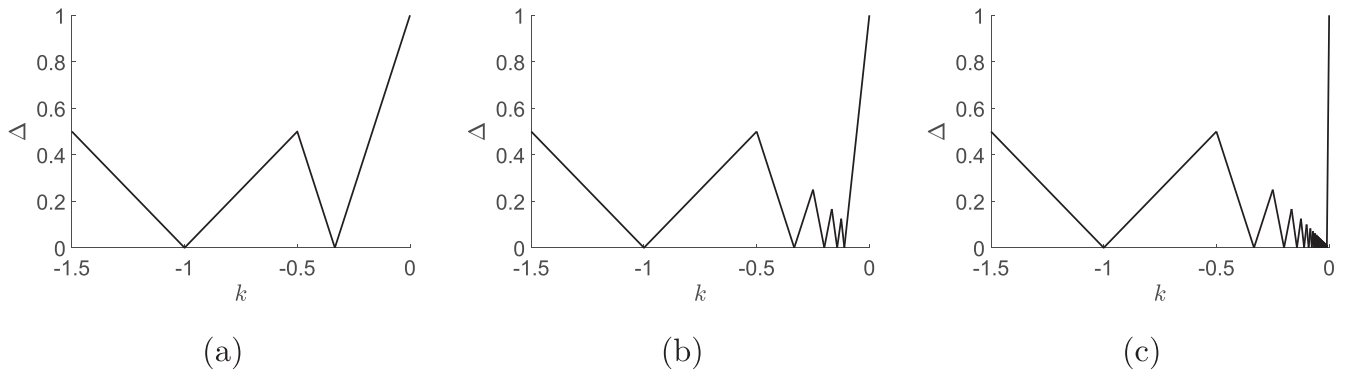


**Figure 3.** Ground-state energy gap  $\Delta$  as a function of  $k$  with  $J = 1$ , and  $\Omega = k/2$ . (a)  $N = 4$ , (b)  $N = 10$ , (c)  $N = 100$ .

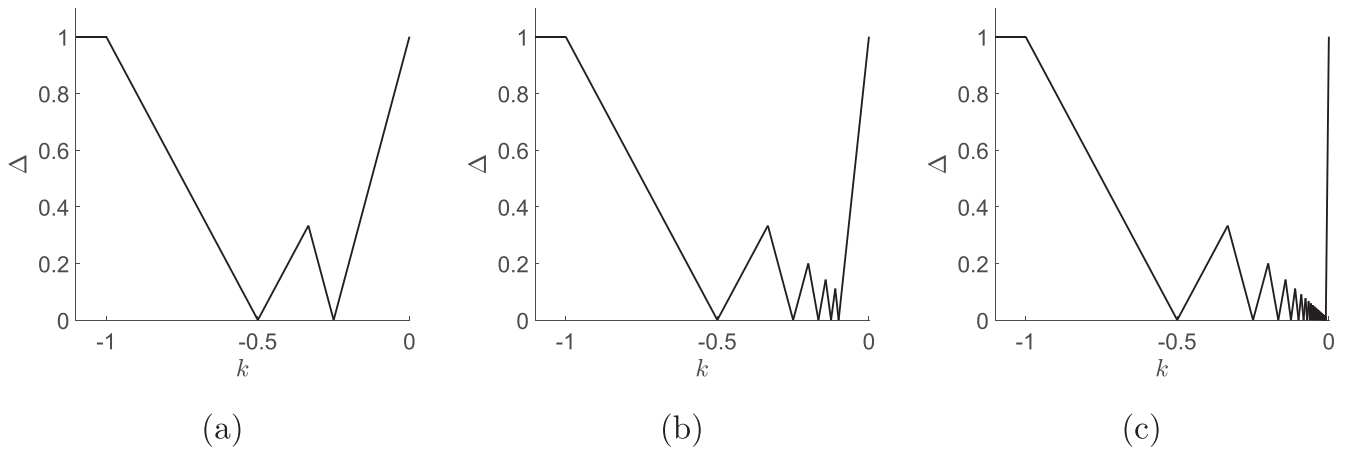


**Figure 4.** Ground-state energy gap  $\Delta$  as a function of  $k$  with  $J = 1$ , and  $\Omega = k/2$ . (a)  $N = 5$ , (b)  $N = 11$ , (c)  $N = 101$ .

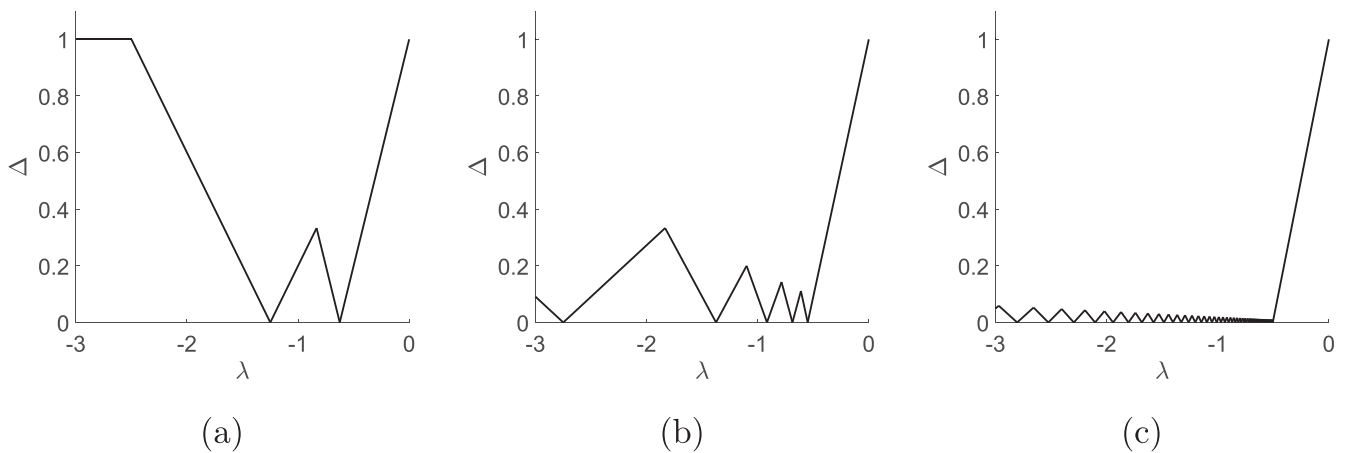


**Figure 5.** Ground-state energy gap  $\Delta$  as a function of  $\lambda$  with  $J = 1$ , and  $\Omega = k/2$ . (a)  $N = 5$ , (b)  $N = 11$ , (c)  $N = 101$ .

For other aspects of the system, however, the number parity effect still has a significant influence. We investigate some further consequences of number parity in the remaining sections.

### 5. Supersymmetry

When  $N$  is even,  $k = J$ , and recalling we have fixed  $\Omega = k/2$ , we observe multiple two-fold degeneracies (note the

energy-level crossings at  $k = 1$  in figure 2(b)) and a single non-degenerate state, the ground state. Consequently, in this case the Hamiltonian possesses supersymmetry (in the sense of supersymmetric quantum mechanics [30, 31]). In particular, the Hamiltonian can be expressed in terms of an anticommutator of supercharges which square to zero. To formalize the result, note that the crossing of energy levels associated with states  $|N, q\rangle$  and  $|N, q'\rangle$  occurs when (11)

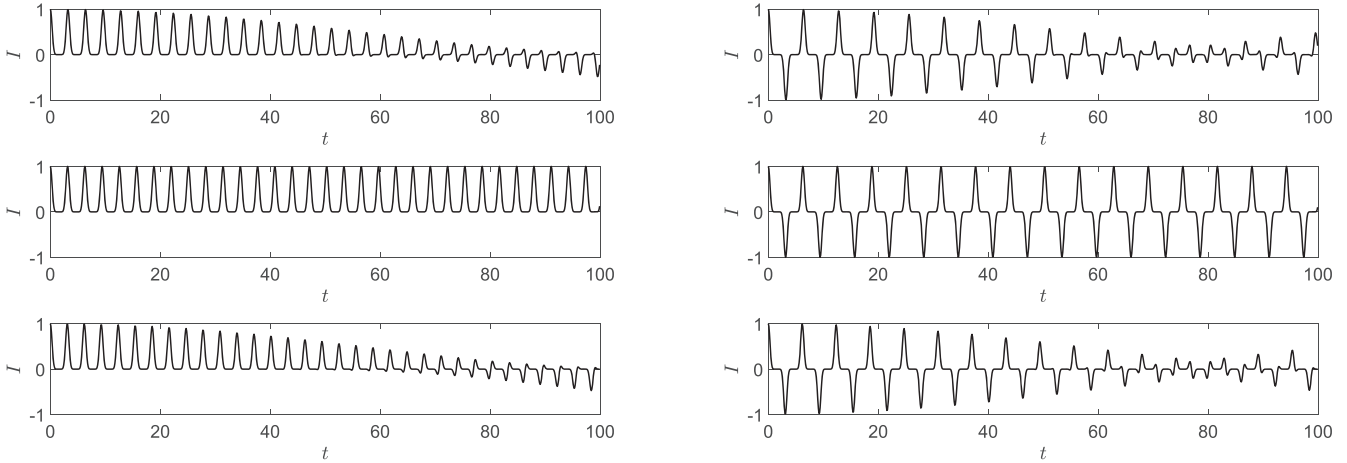


**Figure 6.** Expectation value of the fractional atomic imbalance  $I$  as a function of  $t$  for  $J = 1$  and  $\Omega = k/2$ . On the left,  $N = 10$ , on the right,  $N = 11$ . From top to bottom  $k = \pm 49/50, \pm 1, \pm 51/50$ .

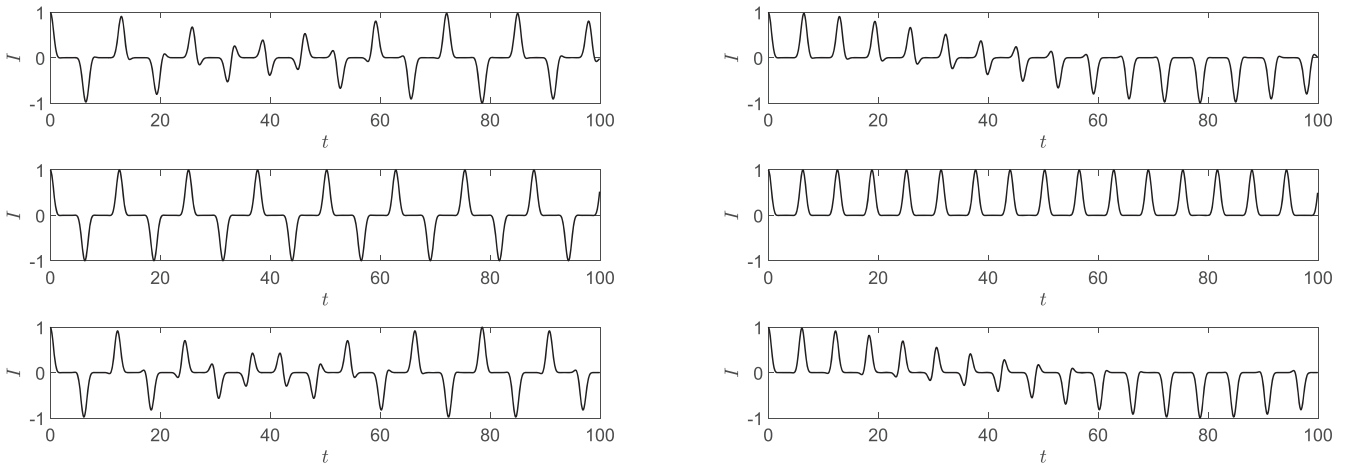


**Figure 7.** Expectation value of the fractional atomic imbalance  $I$  as a function of  $t$  for  $J = 1$  and  $\Omega = k/2$ . On the left,  $N = 10$ , on the right,  $N = 11$ . From top to bottom  $k = \pm 12/25, \pm 1/2, \pm 13/25$ .

holds. Set  $q' = N + 1 - q$  and define

$$Q = \sum_{q=1}^{N/2} \sqrt{qq'} |N, q\rangle \langle N, q'|,$$

$$Q^\dagger = \sum_{q=1}^{N/2} \sqrt{qq'} |N, q'\rangle \langle N, q|.$$

It is easily verified that

$$Q^2 = (Q^\dagger)^2 = 0. \tag{16}$$

Define the Hamiltonian

$$\mathbb{H} = J \left( Q^\dagger Q + Q Q^\dagger - \frac{1}{4} C \right), \tag{17}$$

where  $C$  is the  $su(2)$  Casimir element. Recall that the eigenvalue of  $C$  is  $\Lambda = N(N + 2)/2$ . It is easy to check using only (16) that if  $|\Phi\rangle$  is an eigenstate of (17) with eigenvalue  $E$  then  $Q|\Phi\rangle$  and  $Q^\dagger|\Phi\rangle$  are either eigenvectors with the same eigenvalue, or null vectors. Explicitly

from (17)

$$\begin{aligned} \mathbb{H} &= J \left( -\frac{1}{4} C + \sum_{q=1}^{N/2} qq' (|N, q\rangle \langle N, q| + |N, q'\rangle \langle N, q'|) \right) \\ &= \frac{J}{8} \left( -N(N + 2) |N, 0\rangle \langle N, 0| + \sum_{q=1}^{N/2} (8qq' - N(N + 2)) \right. \\ &\quad \left. \times (|N, q\rangle \langle N, q| + |N, q'\rangle \langle N, q'|) \right) \\ &= \frac{J}{8} \left( \sum_{q=0}^N (8q(N + 1 - q) - N(N + 2)) |N, q\rangle \langle N, q| \right). \end{aligned} \tag{18}$$

Setting  $k = J$  in (10) gives the spectrum of (17), as confirmed by (18).

However, there is no supersymmetry point in the coupling parameter space when  $N$  is odd. One example where this particular parity property has a striking manifestation is in the study of quantum dynamics.

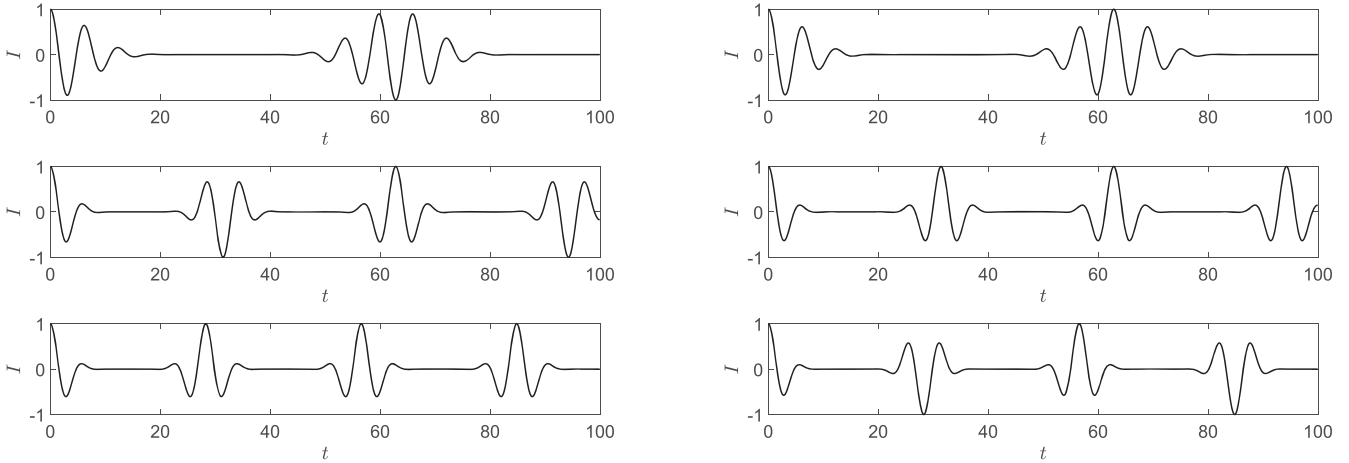


**Figure 8.** Expectation value of the fractional atomic imbalance  $I$  as a function of  $t$  for  $J = 1$  and  $\Omega = k/2$ . On the left,  $N = 10$ , on the right,  $N = 11$ . From top to bottom  $k = \pm 1/20, \pm 1/10, \pm 1/9$ .

### 6. Quantum dynamics

Let

$$|\Phi\rangle = \frac{1}{\sqrt{N!}}(b_1^\dagger)^N|0\rangle,$$

which represents an initial state such that all particles are in the same site. Define the expectation value of the fractional atomic imbalance to be

$$I = N^{-1}\langle\Phi|\exp(iHt)(N_1 - N_2)\exp(-iHt)|\Phi\rangle,$$

where  $t$  denotes time. It can be shown using

$$\langle N, q|\Phi\rangle = \sqrt{\frac{N!}{2^N q!(N - q)!}}$$

that a simple expression for  $I$  is obtained:

$$I = \cos(Jt)(\cos(kt))^{N-1}. \tag{19}$$

At the supersymmetric point  $k = J$  when  $N$  is even, it is apparent that  $0 \leq I \leq 1$ . For odd  $N$  at the same value of coupling parameters it is apparent that  $-1 \leq I \leq 1$ . Thus the even  $N$  case exhibits a type of self-trapping behavior, while the odd  $N$  does not. While the phenomenon of self-trapping is well-known [1, 3], such a parity influence on self-trapping does not appear to have been previously identified.

Since the expression (19) is an even function of  $k$ , exactly the same dynamical behavior occurs for  $k = -J$ . For even  $N$  this corresponds to the smallest value of  $k$  such that the ground-state energy gap is zero. In contrast, for odd  $N$  the smallest value of  $k$  for which the ground-state energy gap is zero is  $k = -J/2$ . Illustrative examples of the expectation values for the fractional atomic imbalance at these parameter values are provided in figures 6 and 7 for  $N = 10$  and  $N = 11$ . It is clear that the number-parity significantly influences the character of the dynamical behavior. This remains true for different parameter values, although the effects are not so pronounced. An example is given in figure 8, with parameter values in the vicinity of  $k = -1/N$  for  $J = 1$ .

### 7. Conclusion

We have studied an extension of the familiar two-site Bose–Hubbard model that includes a second-order tunneling term. This model is known to exhibit three phases determined by fixed-point bifurcations, and in the present work a detailed analysis has been undertaken along a line of the coupling parameter space that includes the boundary between phase-locking and self-trapping phases. All energy levels on this line can be computed analytically, and from this result it was identified that significant number-parity effects are present. In particular, the influence of number-parity on the ground-state energy gap, and the dynamics of the fractional atomic imbalance, were investigated. Our results are applicable in the case of finite value for the coupling  $J$ . Complementary results for the limit as  $J \rightarrow 0$  are provided in [18]. We expect that these analytic results will provide useful consistency checks on non-analytic techniques, in the limit of approaching the self-dual line, in future studies.

Mathematically, the model considered here is equivalent to the Lipkin–Meshkov–Glick (LMG) model of nuclear physics, which can be seen through the spin representation (5). Identification with the generalized LMG model was also adopted in [25–27]. The LMG model been studied through an exact Bethe ansatz solution [32], although the exact solution has a different form to that of [20]. In [32] the analysis was conducted using a choice of coupling parameters such that the region of level crossing is treated as a gapless region in the limit of large particle number. Our results indicate that there may be new insights to be gained for the LMG model, and generalizations, by choosing a different form of coupling parameters. Such an approach has recently been applied to the attractive one-dimensional Bose gas [33]. There, a distinction is made between the zero density thermodynamic limit and the weakly interacting thermodynamic limit, which are obtained by different scaling of parameters as the system size increases.



## Acknowledgments

This research was supported by the Australian Research Council through Discovery Project DP150101294. We thank the mathematical research institute MATRIX in Creswick, Australia, where part of the work was undertaken during the programs *Integrability in low-dimensional quantum systems*, and *Combinatorics, statistical mechanics, and conformal field theory*. We thank Miguel García-March for helpful comments.

## ORCID iDs

Phillip S Isaac  <https://orcid.org/0000-0001-8608-3940>

Jon Links  <https://orcid.org/0000-0003-1049-0616>

## References

- [1] Milburn G J, Corney J, Wright E M and Walls D F 1997 Quantum dynamics of an atomic Bose–Einstein condensate in a double-well potential *Phys. Rev. A* **55** 4318
- [2] Cirac J I, Lewenstein M, Mølmer K and Zoller P 1998 Quantum superposition states of Bose–Einstein condensates *Phys. Rev. A* **57** 1208
- [3] Leggett A J 2001 Bose–Einstein condensation in the alkali gases: some fundamental concepts *Rev. Mod. Phys.* **73** 307
- [4] Kohler S and Sols F 2002 Oscillatory decay of a two-component Bose–Einstein condensate *Phys. Rev. Lett.* **89** 060403
- [5] Zhou H-Q, Links J, McKenzie R H and Guan X-W 2003 Exact results for a tunnel-coupled pair of trapped Bose–Einstein condensates *J. Phys. A: Math. Gen.* **36** L113
- [6] Pan F and Draayer J P 2005 Quantum critical behavior of two coupled Bose–Einstein condensates *Phys. Lett. A* **339** 403
- [7] Albiez M, Gati R, Fölling J, Hunsmann S, Cristiani M and Oberthaler M K 2005 Direct observation of tunneling and nonlinear self-trapping in a single bosonic Josephson junction *Phys. Rev. Lett.* **95** 010402
- [8] Zibold T, Nicklas E, Gross C and Oberthaler M K 2010 Classical bifurcation at the transition from Rabi to Josephson dynamics *Phys. Rev. Lett.* **105** 204101
- [9] Simon L and Strunz W T 2012 Analytical results for Josephson dynamics of ultracold bosons *Phys. Rev. A* **86** 053625
- [10] Graefe E-M, Korsch H J and Strzys M P 2014 Bose–Hubbard dimers, Viviani’s windows and pendulum dynamics *J. Phys. A: Math. Theor.* **47** 085304
- [11] Pérez-Campos C, González-Alonso J R, Castañón O and López-Peña R 2010 Entanglement and localization of a two-mode Bose–Einstein condensate *Ann. Phys.* **325** 325
- [12] Rubeni D, Foerster A, Mattei E and Roditi I 2012 Quantum phase transition in Bose–Einstein condensate from a Bethe ansatz perspective *Nucl. Phys. B* **856** 698
- [13] Buonsante P, Burioni R, Vescovi E and Vezzani A 2012 Quantum criticality in a bosonic Josephson junction *Phys. Rev. A* **85** 043625
- [14] Julia-Diaz B, Martorell J and Polls A 2010 Bose–Einstein condensates on slightly asymmetric double-well potentials *Phys. Rev. A* **81** 063625
- [15] Sakmann K, Streltsov A I, Alon O E and Cederbaum L S 2014 Universality of fragmentation in the Schrödinger dynamics of bosonic Josephson junctions *Phys. Rev. A* **89** 023602
- [16] Auccaise R, Araujo-Ferreira A G, Sarthour R S, Oliveira I S, Bonagamba T J and Roditi I 2015 Spin squeezing in a quadrupolar nuclei NMR system *Phys. Rev. Lett.* **114** 043604
- [17] Links J and Marquette I 2015 Ground-state Bethe root densities and quantum phase transitions *J. Phys. A: Math. Theor.* **48** 045204
- [18] Liang J-Q, Liu J-L, Li W-D and Li Z-J 2009 Atom-pair tunneling and quantum phase transition in the strong-interaction regime *Phys. Rev. A* **79** 033617
- [19] Cao H and Fu L B 2012 Quantum phase transition and dynamics induced by atom-pair tunnelling of Bose–Einstein condensates in a double-well potential *Eur. Phys. J. D* **66** 97
- [20] Rubeni D, Links J, Isaac P S and Foerster A 2017 Two-site Bose–Hubbard model with nonlinear tunneling: classical and quantum analysis *Phys. Rev. A* **95** 043607
- [21] Ananikian D and Bergeman T 2006 Gross–Pitaevskii equation for Bose particles in a double-well potential: two-mode models and beyond *Phys. Rev. A* **73** 013604
- [22] Gati R and Oberthaler M K 2007 A bosonic Josephson junction *J. Phys. B: At. Mol. Opt. Phys.* **40** R61
- [23] Fölling S, Trotzky S, Cheinet P, Feld M, Saers R, Widera A, Müller T and Bloch I 2007 Direct observation of second-order atom tunnelling *Nature* **448** 1029
- [24] Links J and Zhao S-Y 2009 A Bethe ansatz study of the ground state energy for the repulsive Bose–Hubbard dimer *J. Stat. Mech.* **P03013**
- [25] García-March M A, Dounas-Frazer D R and Carr L D 2011 Macroscopic superposition of ultracold atoms with orbital degrees of freedom *Phys. Rev. A* **83** 043612
- [26] García-March M A, Dounas-Frazer D R and Carr L D 2012 Macroscopic superposition states of ultracold bosons in a double-well potential *Front. Phys.* **7** 131
- [27] García-March M A and Carr L D 2015 Vortex macroscopic superpositions in ultracold bosons in a double-well potential *Phys. Rev. A* **91** 033626
- [28] Zürn G, Wenz A N, Murmann S, Bergschneider A, Lompe T and Jochim S 2013 Pairing in few-fermion systems with attractive interactions *Phys. Rev. Lett.* **111** 175302
- [29] Schilling C and Schilling R 2016 Number-parity effect for confined fermions in one dimension *Phys. Rev. A* **93** 021601
- [30] Cooper F, Khare A and Sukhatme U 1995 Supersymmetry and quantum mechanics *Phys. Rep.* **251** 267
- [31] Witten E 1981 Dynamical breaking of supersymmetry *Nucl. Phys. B* **185** 513
- [32] Lerma H S and Dukelsky J 2013 The Lipkin–Meshkov–Glick model as a particular limit of the  $SU(1, 1)$  Richardson–Gaudin integrable models *Nucl. Phys. B* **870** 421
- [33] Piroli L and Calabrese P 2016 Local correlations in the attractive one-dimensional Bose gas: from Bethe ansatz to the Gross–Pitaevskii equation *Phys. Rev. A* **94** 053620